

How do Hydrological Variability and Human Activities Control the Spatiotemporal Changes of Riverine Nitrogen Export in the Upper Mississippi River Basin?

Qianyu Zhao, Bin Peng,* Zewei Ma, Mengqi Jia, Gregory F. McIsaac, Dale M. Robertson, David A. Saad, Richard E. Warner, Xiaocui Wu, Qu Zhou, and Kaiyu Guan*



Cite This: <https://doi.org/10.1021/acs.est.5c06476>



Read Online

ACCESS |

Metrics & More

Article Recommendations

Supporting Information

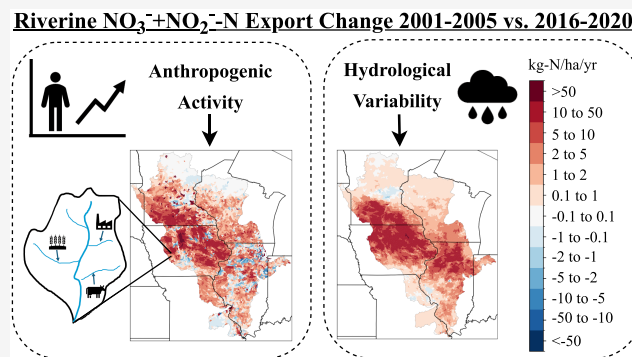
ABSTRACT: Excessive nitrogen export from agricultural watersheds remains a critical water quality challenge, with the Upper Mississippi River Basin (UMRB) significantly contributing to downstream eutrophication and hypoxia in the Gulf. This study investigates the spatiotemporal dynamics of riverine nitrate plus nitrite ($\text{NO}_3^- + \text{NO}_2^-$ -N) export across the UMRB at high spatial resolution (12-digit Hydrologic Unit Codes or HUC12 subwatershed scale) during 2001–2020 and quantifies the effects of anthropogenic activities and hydrological variability on riverine $\text{NO}_3^- + \text{NO}_2^-$ -N export changes in the region between 2001–2005 and 2016–2020. Our results revealed hotspots of substantial increases in $\text{NO}_3^- + \text{NO}_2^-$ -N yields across the UMRB, with distinct regional patterns in driving factors. Over the entire UMRB, $\text{NO}_3^- + \text{NO}_2^-$ -N yields increased by 9.7 kg/ha/yr on average from 2001–2005 to 2016–2020, with anthropogenic activities contributing 4.8 kg/ha/yr and hydrological variability contributing 4.9 kg/ha/yr. The northern and western UMRB had combined influences from both anthropogenic activities and hydrological variability, while the east-central regions had predominantly hydrologically driven changes. Agricultural sources, including fertilizer, manure, and biological nitrogen fixation, collectively contributed over 80% of $\text{NO}_3^- + \text{NO}_2^-$ -N loading throughout the basin. This framework for disentangling human and hydrological impacts provides critical insights for developing effective and targeted watershed management strategies to reduce nutrient losses and improve water quality.

KEYWORDS: nutrient export, nitrogen export yield, upper mississippi river basin, WRTDS-K, SPARROW, anthropogenic impact, hydrological impact

1. INTRODUCTION

Excessive nutrient export, especially nitrogen export, is one of the most pressing water quality problems and has cascading effects on aquatic ecosystems and human health across the globe.^{1–16} The Upper Mississippi River Basin (UMRB) is a major contributor of nitrogen to the Mississippi-Atchafalaya River Basin (MARB) and ultimately to the Gulf, significantly impacting coastal ecosystems.^{11,17–23} Despite ongoing state and regional nutrient reduction efforts across the UMRB, limited understanding of spatiotemporal changes and driving factors of riverine nutrient exports at high resolutions hinders the development of effective policy design and targeted watershed management.^{11,24–29}

From a practical viewpoint, local hydrologic units, such 12-digit Hydrologic Unit Codes (HUC12, ~25–100 km²) defined by the U.S. Geological Survey (USGS), represent a critical management unit, effectively balancing the capture of heterogeneous land use and hydrologic processes with computational efficiency while providing actionable context



for stakeholders.^{30–32} Despite extensive research using various modeling approaches to understand nutrient transport across multiple scales in the UMRB, from regional basin-scale^{33–37} to HUC08 scale³⁸ to field scale,^{18,39} and from process-based hydrological models (Soil and Water Assessment Tool, SWAT),⁴⁰ to semiempirical models (Spatially Referenced Regression On Watershed attributes, SPARROW),¹¹ to machine learning methods,⁴¹ critical knowledge gaps of nutrient spatiotemporal dynamics persist at the regional scale and at the HUC12-level resolution, particularly in quantifying the interactions between nutrient inputs, transport processes, and hydrological dynamics.⁴²

Received: May 14, 2025

Revised: December 1, 2025

Accepted: December 2, 2025

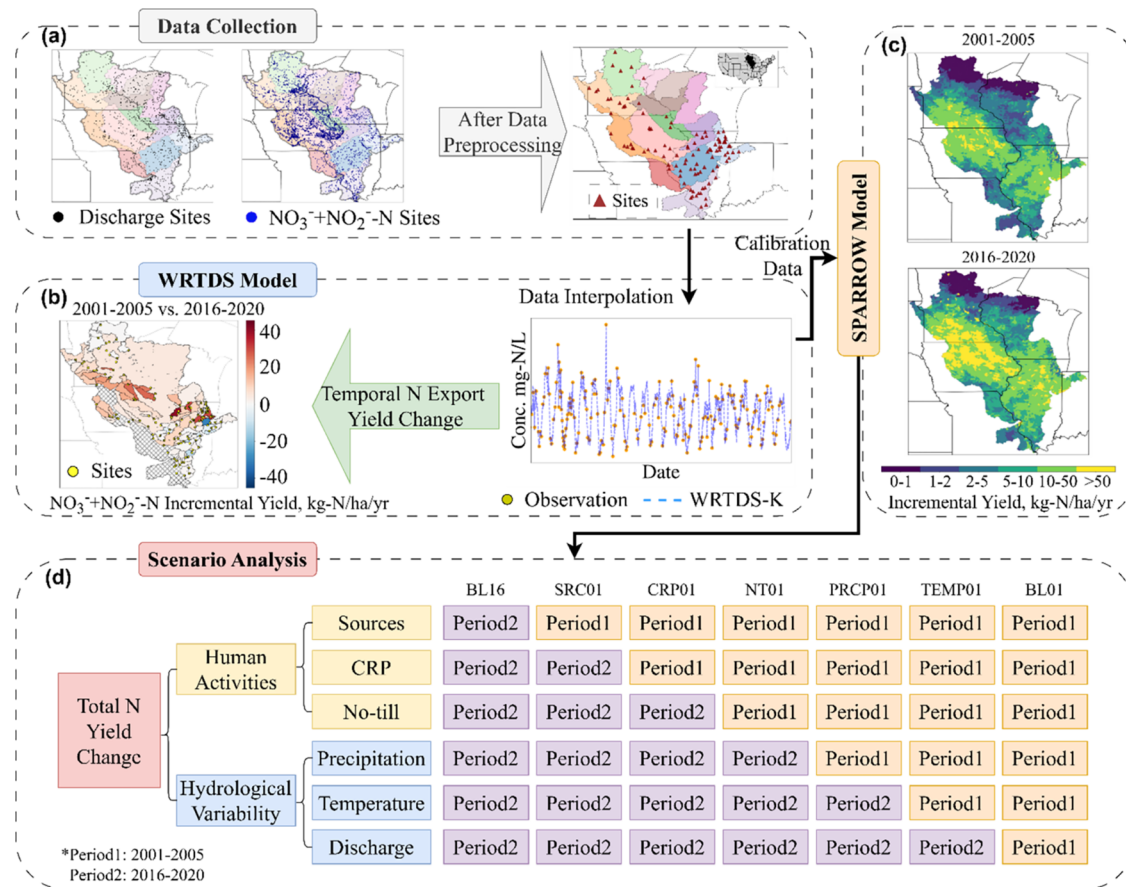


Figure 1. Methodological workflow for analyzing spatiotemporal changes in the $\text{NO}_3^- + \text{NO}_2^-$ -N export. (a) Data collection and preprocessing from discharge and $\text{NO}_3^- + \text{NO}_2^-$ -N monitoring sites. Inset: Spatial extent of the Upper Mississippi River Basin (UMRB). (b) Implementation of WRTDS-K to estimate annual $\text{NO}_3^- + \text{NO}_2^-$ -N loads and yields. (c) The spatial $\text{NO}_3^- + \text{NO}_2^-$ -N export patterns for two time periods (2001–2005 and 2016–2020) estimated with the SPARROW model. (d) Scenario design to separate anthropogenic impact and hydrologic impact on $\text{NO}_3^- + \text{NO}_2^-$ -N export.

Besides identifying spatiotemporal patterns, understanding and quantifying the impacts of the underlying drivers of these patterns are important for developing effective mitigation strategies for nutrient loss. A key challenge in nutrient export research is the lack of a scalable, spatially detailed, and temporally consistent framework for attributing changes to distinct drivers. Previous efforts to differentiate these impacts have primarily been conducted at the basin scale using data-driven approaches (N budgets,⁴³ flow normalization,⁴⁴ and land-use categorization⁴⁵) or at small watershed scales using process-based models like SWAT.⁴⁶ There remains a critical gap in quantifying the effects of anthropogenic activities (e.g., fertilizer application) and natural hydrological variability (e.g., precipitation) on nitrogen export, particularly at fine spatial resolutions across large regions and over extended time periods. To fill this gap, this study proposed a scenario-based modeling approach that integrates long-term datasets with an annual-scale SPARROW model, effectively differentiating the anthropogenic and hydrological contributions. This study is the first comprehensive spatiotemporal analysis of $\text{NO}_3^- + \text{NO}_2^-$ -N export at the HUC12 resolution across the UMRB over a 20-year period (2001–2020).

The overarching goal of this study was to investigate the changes and driving factors of the $\text{NO}_3^- + \text{NO}_2^-$ -N yields and quantify the effects of anthropogenic activities and hydrological variability. $\text{NO}_3^- + \text{NO}_2^-$ -N represents the mobile and

bioavailable forms of nitrogen most relevant to aquatic ecosystem impacts and the type of nitrogen most commonly measured. This study addresses three key science questions regarding $\text{NO}_3^- + \text{NO}_2^-$ -N dynamics: What are the spatiotemporal patterns of the $\text{NO}_3^- + \text{NO}_2^-$ -N export in the UMRB? What factors are shaping the patterns of the $\text{NO}_3^- + \text{NO}_2^-$ -N export? How and to what extent did anthropogenic activity and hydrological variability affect the $\text{NO}_3^- + \text{NO}_2^-$ -N export? This study aims to support targeted nutrient reduction strategies and provides a replicable framework for investigating nutrient dynamics over a range of spatial scales in large river systems.

2. METHODS AND DATA

To address these questions, this study employed a systematic methodological framework (Figure 1). WRTDS-K (Weighted Regressions on Time, Discharge, and Season with Kalman Filtering, developed by USGS)⁴⁸ was used to estimate annual $\text{NO}_3^- + \text{NO}_2^-$ -N loads from 2001 to 2020 at monitoring stations. These estimated loads were used to calibrate the annual-scale SPARROW model, developed by the USGS,^{49,50} which was used to quantify spatial and temporal changes in $\text{NO}_3^- + \text{NO}_2^-$ -N export in the UMRB. A scenario analysis was then conducted by comparing model outputs from two five-year periods, 2001–2005 and 2016–2020, to differentiate the effects of anthropogenic and hydrological drivers.

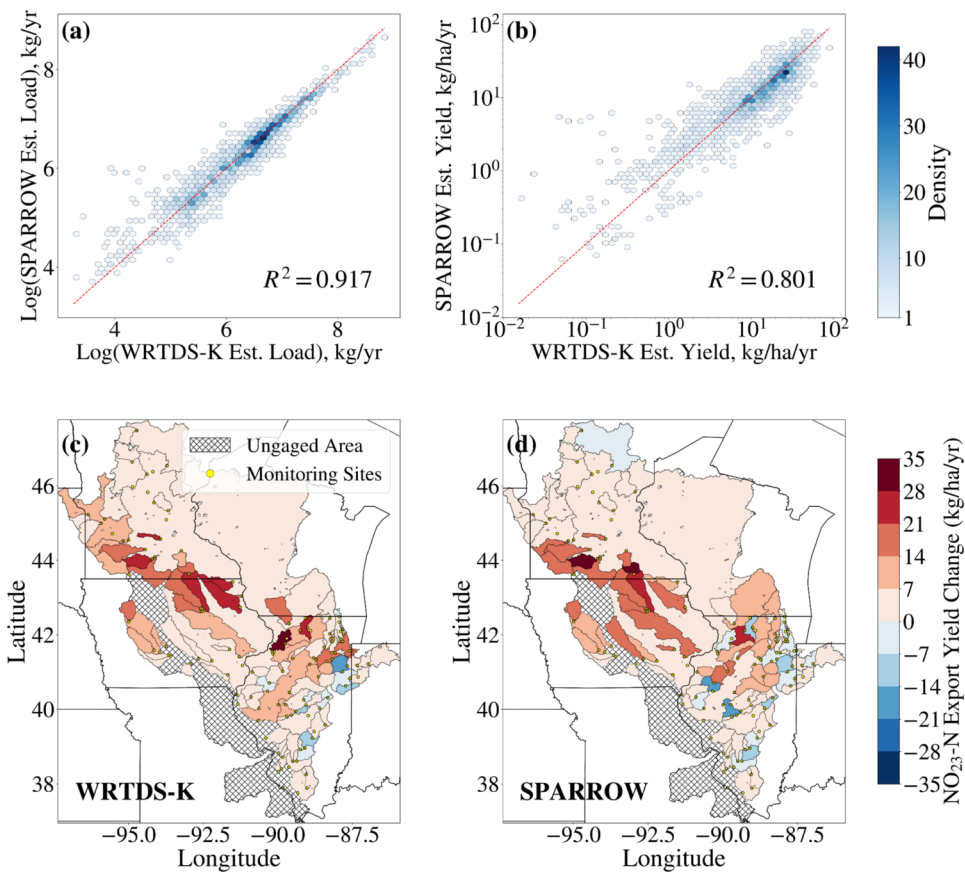


Figure 2. Calibration results for the SPARROW model compared with the observed (WRTDS-K estimated) annual loads. Panels (a, b) show the SPARROW performance for $\text{NO}_3^- + \text{NO}_2^-$ -N export loads (a) and yields (b) at 104 USGS gaging stations, with R^2 values of 0.917 and 0.801, respectively. Panels (c, d) show the spatial distribution of incremental $\text{NO}_3^- + \text{NO}_2^-$ -N yield changes in the UMRB estimated by WRTDS-K and the SPARROW model, respectively, validating the performance of the SPARROW model (calculation described in the [Supporting Information Text S2](#)). Both WRTDS-K estimated and SPARROW modeled results show substantial $\text{NO}_3^- + \text{NO}_2^-$ -N yield increases in the northern portions of the UMRB. The strong spatial agreement between WRTDS-K and SPARROW estimations and statistical results validates the reliability of the $\text{NO}_3^- + \text{NO}_2^-$ -N yield predictions with the SPARROW model.

2.1. Study Region. Located in the Midwest region of the U.S., the UMRB encompasses approximately 492,000 km² across primarily Minnesota, Wisconsin, Iowa, Illinois, and Missouri, representing one of North America's most significant agricultural regions, as shown in [Figure S1](#). In the UMRB, agriculture, primarily corn and soybeans, accounts for nearly half (49.4%) of the land. The remaining area consists of forests (19.2%), wetlands and waterbodies (11.6%), pasture and hay fields (9.8%), and urban development (9.1%).^{30,47}

2.2. The SPARROW Model. This study used the R implementation of the SPAtially Referenced Regressions On Watershed attributes (SPARROW) model (RSPARROW, version 1.1.0), a hybrid empirical/process-based watershed modeling framework that relates stream nutrient loads to spatially referenced catchment characteristics, including nutrient sources, land-to-water delivery factors, and in-stream decay processes. More details about the SPARROW model and source code are provided in the Supporting Information ([Text S1](#)).

Unlike earlier SPARROW applications that focused on long-term mean annual conditions, this study applied the model using an annual time step. As a result, the SPARROW predictions represent annual conditions rather than long-term means, enabling spatiotemporal tracking of the nutrient dynamics. The SPARROW model was calibrated using a 20-

year dataset of 2080 WRTDS-K estimated annual $\text{NO}_3^- + \text{NO}_2^-$ -N loads from 104 monitoring stations ([Table S5](#)). Additional details about WRTDS-K and the SPARROW model inputs are provided in the Supporting Information ([Text S2–S3 and Table S1](#)). The calibrated SPARROW model was then used to simulate annual $\text{NO}_3^- + \text{NO}_2^-$ -N loads and yields across all HUC12s, including ungaaged areas.

2.3. Model Performance Evaluation and Validation. To evaluate the SPARROW model's generalizability and robustness, this study implemented a three-way cross-validation approach, including spatial validation (spatially divided monitoring sites), temporal validation (temporally partitioned the 20-year study period), and random validation (randomly subdivided the observations). Details of the procedure are provided in the Supporting Information ([Text S4](#)).

The SPARROW model's predictive capability was evaluated using the coefficient of determination (R^2) and root mean squared error (RMSE) metrics to quantify model fitting. Both conditioned and unconditioned model results were reported. In the conditioned mode (used for model calibration), the SPARROW model adjusts the load to the measured load before predicting further downstream loads, whereas the unconditioned mode (used for model predictability) relies solely on model simulation without such load adjustments.

2.4. Scenario-Based Attribution Framework. To separate anthropogenic and hydrological effects on $\text{NO}_3^- + \text{NO}_2^-$ -N yields over time, a scenario analysis framework was designed (Figure 1d and Table S2). Anthropogenic factors include all nitrogen sources and conservation practices, while hydrological factors contain weather-related variables. Two specific five-year windows (2001–2005 and 2016–2020) were selected to characterize $\text{NO}_3^- + \text{NO}_2^-$ -N transport patterns during relatively stable periods by minimizing interannual variability while providing sufficient temporal distance to detect shifts in land use, conservation practices, and hydrology trends. To ensure the robustness of our findings, alternative temporal configurations were tested (e.g., 2001–2006 vs 2015–2020, 2001–2007 vs 2014–2020, 2001–2008 vs 2013–2020, 2001–2009 vs 2012–2020, and 2001–2010 vs 2011–2020) and had similar spatial patterns. Therefore, we report the results from only these two periods here.

Two baseline scenarios established temporal reference points: BL16 (2016–2020 levels) and BL01 (2001–2005 levels) (full change through time). Intermediate scenarios systematically modified variables to isolate specific effects: scenario SRC01 adopted 2001–2005 sources with 2016–2020 all other management actions, land-to-water delivery, and attenuation conditions. In CRP01 (all sources and CRP implementation during the first period), NT01 (sources, CRP, and no-till during the first period), PRCP01 (all anthropogenic factors and precipitation during the first period), and TEMP01 (all anthropogenic factors, precipitation, and temperature during the first period), we sequentially changed one variable to its 2001–2005 level. Each scenario ran over a 5-year period, and the results were averaged.

The HUC12-level changes in $\text{NO}_3^- + \text{NO}_2^-$ -N yields were calculated by differencing scenario outputs (such as BL16–BL01 for all factors) and just all anthropogenic impacts (BL16–NT01) and just all hydrological impacts (NT01–BL01). Individual variable impacts were quantified for nitrogen sources (BL16–SRC01), CRP implementation (SRC01–CRP01), no-till practices (CRP01–NT01), annual total precipitation (NT01–PRCP01), temperature (PRCP01–TEMP01), and discharge (TEMP01–BL01), where discharge affects nutrient in-channel attenuation. More details about scenario description and simulation logic are provided in the Supporting Information (Text S5).

3. RESULTS

3.1. SPARROW Model Results. **3.1.1. SPARROW Calibration and Validation.** The scatter plots in Figure 2a,b show the calibration results, comparing SPARROW estimated $\text{NO}_3^- + \text{NO}_2^-$ -N loads and yields against WRTDS-K estimates. The calibration had a conditioned R^2 of 0.917 and an RMSE of 0.561 for $\text{NO}_3^- + \text{NO}_2^-$ -N loads (Figure 2a), and an R^2 of 0.801 for $\text{NO}_3^- + \text{NO}_2^-$ -N yields (Figure 2b). The unconditioned (full prediction) R^2 was 0.903 and RMSE was 0.609 for loads with an R^2 of 0.765 for yields.

The strong spatial agreement between WRTDS-K (observed) and SPARROW predictions (Figures 2c,d and S2) demonstrates SPARROW's reliability. To further assess model generalizability, three distinct 5-fold cross-validation approaches were implemented (Table S4). The spatial validation approach, testing spatial extrapolation capabilities, had average unconditioned validation R^2 's of 0.866 for loads and 0.685 for yields. Temporal validation, assessing the temporal extrapolation ability, had average unconditioned validation R^2 's of

0.896 for loads and 0.746 for yields. The random validation approach, testing overall model robustness, had average unconditioned validation R^2 's of 0.902 for loads and 0.764 for yields. These consistently high-performance metrics across all validation approaches demonstrate the model's reliability for both spatial and temporal applications.

3.1.2. SPARROW Model Coefficients. All of the coefficients in the model were statistically significant ($p < 0.05$), as shown in Table S3. To transform the model outputs from the log scale to real-world units, the source coefficients were multiplied by the mean exponentiated weighted error (MEWE).¹¹

The coefficients for the sources indicate the amount (as a percentage of the input for inputs defined in kg/yr or a rate of delivery for inputs defined as an aerial coverage) of $\text{NO}_3^- + \text{NO}_2^-$ -N possibly entering the waterbodies under the mean land-to-water delivery condition for the entire area. Wastewater treatment plants (WWTP) had a coefficient of 0.589 (95% confidence interval (CI): 0.514–0.664), indicating that each estimated kilogram of total nitrogen discharge contributes 0.683 kg (0.589×1.160 MEWE) of $\text{NO}_3^- + \text{NO}_2^-$ -N input. Other significant source contributions include wet inorganic nitrogen (including NH_4^+ and NO_3^-) atmospheric deposition (coefficient: 0.208, 95% CI: 0.134–0.281) contributing 0.241 kg of $\text{NO}_3^- + \text{NO}_2^-$ -N per kg-N input, manure (coefficient: 0.181, 95% CI: 0.141–0.221) contributing 0.210 kg of $\text{NO}_3^- + \text{NO}_2^-$ -N per kg-N input, and fertilizer (coefficient: 0.037, 95% CI: 0.024–0.050) contributing 0.043 kg of $\text{NO}_3^- + \text{NO}_2^-$ -N per kg-N input. Because atmospheric deposition was estimated by only wet deposition that represents about 50% of the total input; therefore, total atmospheric deposition contributes ~ 0.121 kg of $\text{NO}_3^- + \text{NO}_2^-$ -N per kg-N input. Land use sources also had significant effects, with biological nitrogen fixation (BNF) contributing 645 kg- $\text{NO}_3^- + \text{NO}_2^-$ -N/km²/yr (coefficient: 556, 95% CI: 292–821) and urban nonpoint sources contributing 181 kg- $\text{NO}_3^- + \text{NO}_2^-$ -N/km²/yr (coefficient: 156, 95% CI: 103–209) to $\text{NO}_3^- + \text{NO}_2^-$ -N input.

The land-to-water delivery coefficients quantify how watershed characteristics affect the transport of nitrogen from the land to water. Tile drainage had a significant positive coefficient (+0.032, 95% CI: 0.030–0.034), indicating enhanced $\text{NO}_3^- + \text{NO}_2^-$ -N delivery in higher tiled areas. Precipitation also exhibited a positive relationship (+0.0017, 95% CI: 0.0015–0.0019), indicating that more $\text{NO}_3^- + \text{NO}_2^-$ -N will be delivered to the river system with additional precipitation from the standardized status. Conversely, temperature had a negative coefficient (-0.032 , 95% CI: $-0.049 - -0.015$), with higher temperature reducing $\text{NO}_3^- + \text{NO}_2^-$ -N delivery. Clay content in soil had a positive effect (+0.004, 95% CI: 0.0002–0.0079) on $\text{NO}_3^- + \text{NO}_2^-$ -N delivery, which may reflect that reduced infiltration and increased surface runoff in clay-rich soils enhance nitrogen transport to streams. Greater CRP (-0.068 , 95% CI: $-0.085 - -0.051$) area reduces $\text{NO}_3^- + \text{NO}_2^-$ -N transport in the UMRB, while higher adoption of no-till (0.011, 95% CI: 0.009–0.0013) practices facilitated $\text{NO}_3^- + \text{NO}_2^-$ -N transport in the UMRB.

The attenuation coefficients capture the loss of $\text{NO}_3^- + \text{NO}_2^-$ -N, such as denitrification, biological uptake, and sedimentation that remove $\text{NO}_3^- + \text{NO}_2^-$ -N during in-stream and in-reservoir transport. Stream attenuation (0.060, 95% CI: 0.049–0.071) represents the mean rate at which $\text{NO}_3^- + \text{NO}_2^-$ -N is removed from the stream per unit of travel time

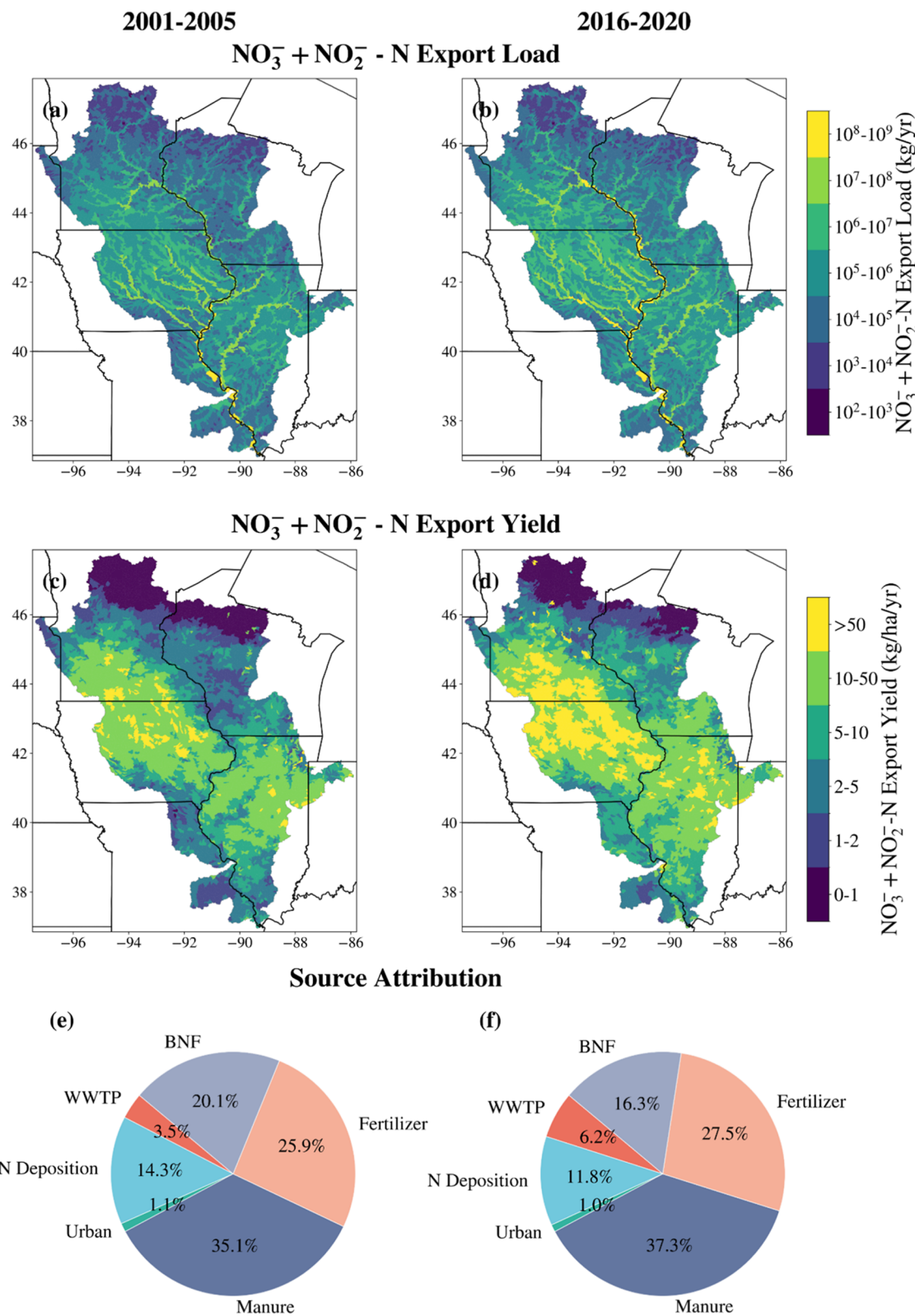


Figure 3. Spatial distribution of SPARROW simulated $\text{NO}_3^- + \text{NO}_2^-$ -N loads (panels (a, b)) and local yields generated within each 12-digit Hydrologic Unit Code (HUC12) (panels (c, d)) in the UMRB for two time periods: 2001–2005 Panel (a, c) and 2016–2020 (Panel (b, d)). The patterns in $\text{NO}_3^- + \text{NO}_2^-$ -N loads show consistent spatial distribution along major waterways, while patterns in yields demonstrate significant intensification in agricultural regions, particularly in southern Minnesota and northern Iowa, during the 2016–2020 period. Estimated relative contributions of different nitrogen sources to $\text{NO}_3^- + \text{NO}_2^-$ -N incremental loads at HUC12 local outlets in the UMRB during (e) 2001–2005 and (f) 2016–2020 periods. Sources include fertilizer, manure, atmospheric deposition (N Deposition), biological nitrogen fixation (BNF), wastewater treatment plants (WWTP), and urban nonpoint sources (Urban).

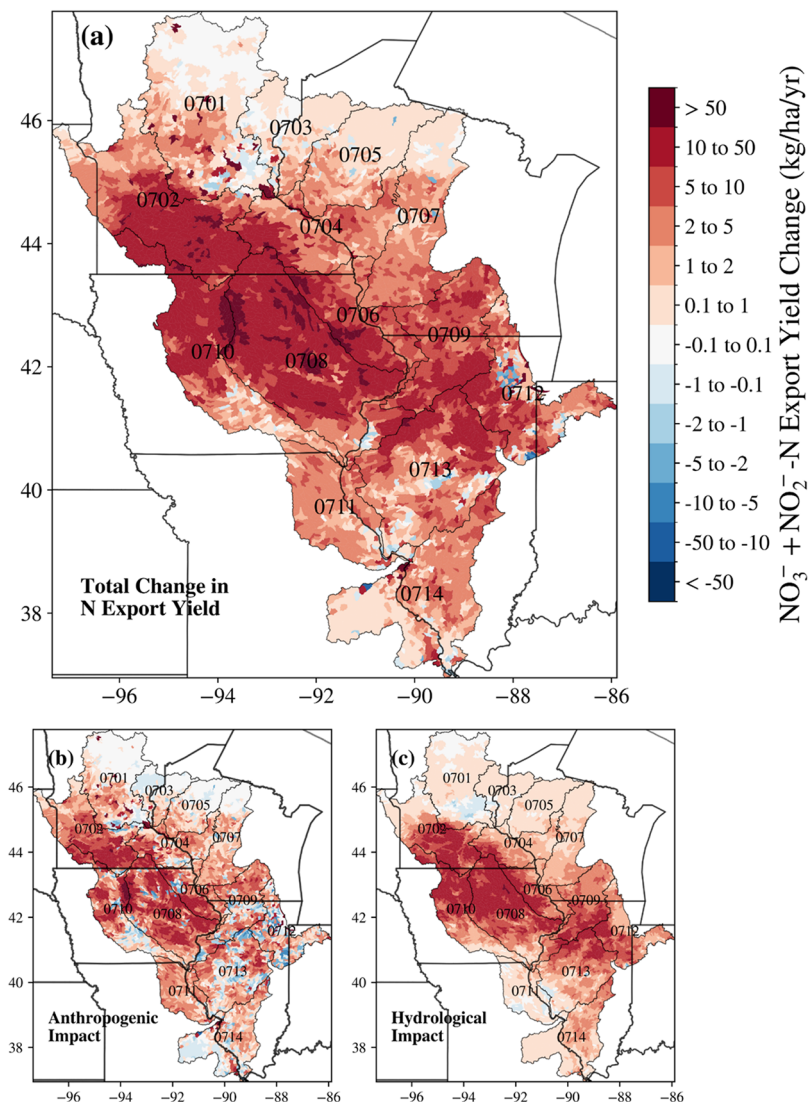


Figure 4. Spatial decomposition of changes in $\text{NO}_3^- + \text{NO}_2^-$ -N yields (kg/ha/yr) in the UMRB from (a) total change (BL16-BL01) into (b) anthropogenic effects (BL16-NT01), and (c) hydrological effects (NT01-BL01). Results are shown at the HUC12 resolution with HUC4 boundaries overlaid for reference. Total yields increased significantly in HUC numbers 0702, 0706, 0708, 0709, 0710, and 0712. Anthropogenic impacts show stronger positive influences particularly in HUC 0702, 0706, 0708, and 0710, while hydrological impacts led to a significant increase in 0702, 0710, 0708, 0709, and 0712.

divided by water depth, indicating that longer travel times result in greater $\text{NO}_3^- + \text{NO}_2^-$ -N removal. Reservoir attenuation (3.481, 95% CI: 2.205–4.757) describes the $\text{NO}_3^- + \text{NO}_2^-$ -N retention in lakes and reservoirs, meaning that reservoirs with longer mean residence time provide more $\text{NO}_3^- + \text{NO}_2^-$ -N removal.

3.2. Spatiotemporal Changes of Riverine $\text{NO}_3^- + \text{NO}_2^-$ -N Export Across the UMRB. The spatial distribution in loads was very similar in 2001–2005 and 2016–2020, with the largest loads during both time periods in the major rivers (Figure 3a,b). $\text{NO}_3^- + \text{NO}_2^-$ -N yield distributions (Figure 3c,d) in 2001–2005 and 2016–2020 had more spatial variation, highlighting watershed-specific differences in $\text{NO}_3^- + \text{NO}_2^-$ -N export.

3.2.1. Spatiotemporal Trend Patterns. In the UMRB, the $\text{NO}_3^- + \text{NO}_2^-$ -N yield hotspots were predominantly located in the central part of the basin, specifically in southern Minnesota, northern Iowa, and northern Illinois (Figure 3c,d). In the west-central and eastern UMRB, the $\text{NO}_3^- + \text{NO}_2^-$ -N yields

increased significantly in 2016–2020 compared to 2001–2005, reflecting intensified agricultural activities^{51,52} and increases in precipitation.⁵³ In addition, the $\text{NO}_3^- + \text{NO}_2^-$ -N yields delivered to the outlet of the UMRB shown in Figure S3 also increased in the same regions with the highest incremental yields. The fraction of incremental (i.e., local contributions independent of further upstream inputs) $\text{NO}_3^- + \text{NO}_2^-$ -N load delivered to the outlet (Figure S4) further emphasizes the importance of proximity to major waterways with areas closer to the main stem having higher delivery ratios. These spatial patterns demonstrate the complex interaction between nitrogen sources, hydrological connectivity, and nitrogen attenuation processes across the basin.

3.2.2. Source Attributions. The $\text{NO}_3^- + \text{NO}_2^-$ -N source contributions to the streams were estimated by the SPARROW model as shown in Figure 3e,f, which represent the 2001–2005 and 2016–2020 periods, respectively. The contributions of incremental loads delivered to the outlet of the UMRB are shown in Figure S5. As shown in Figure 3e, during 2001–

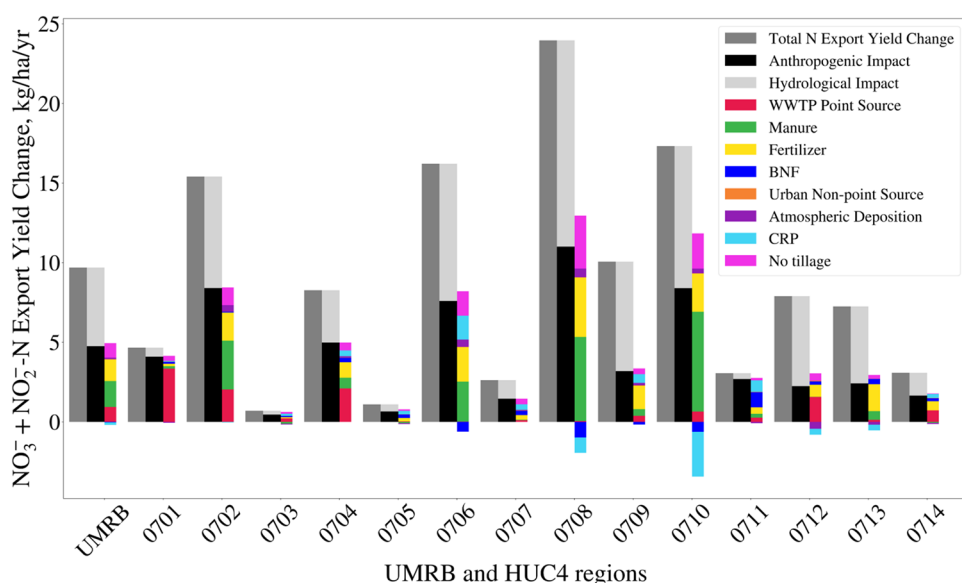


Figure 5. Decomposition of $\text{NO}_3^- + \text{NO}_2^-$ -N yield changes (kg/ha/yr) across the UMRB and its HUC4 subregions.

2005, manure was the largest nitrogen source contributor (35.1%), followed closely by fertilizer application (25.9%), BNF (20.1%), and atmospheric deposition (14.3%). Urban point (WWTP) and nonpoint sources collectively account for 4.6%.

Compared to the 2001–2005 period, several changes in source contributions happened during the 2016–2020 later period, as shown in Figure 3f. Fertilizer and manure contributions increased from 25.9% and 35.1% to 27.5% and 37.3%, respectively, and remained the dominant nitrogen sources. Atmospheric nitrogen deposition exhibited a decrease in relative contribution from 14.3% to 11.8%, but with an increase in the absolute value from 8.7×10^7 to 1.3×10^8 kg-N/yr. Urban source contributions increased from 4.6% to 7.2%, indicating a growing urban influence on basin-wide $\text{NO}_3^- + \text{NO}_2^-$ -N loads. The sum of all the sources had increased in their absolute values of the sum of 5-year average annual $\text{NO}_3^- + \text{NO}_2^-$ -N incremental loads in the UMRB (Figure S6), suggesting a greater need for targeted management strategies that reduce both point and nonpoint sources. The incremental source contributions delivered to the outlet of the UMRB (Figures S5 and S7) exhibit patterns similar to the contribution of HUC12 incremental loads.

3.3. Disentangling the Impacts of Hydrological Variability and Anthropogenic Activities. Decomposition of the overall changes in $\text{NO}_3^- + \text{NO}_2^-$ -N yields into those caused by anthropogenic effects (BL16-NT01) and hydrological effects (NT01-BL01) had significant spatial variability across the UMRB (Figure 4). The human impact scenario (BL16-NT01) with impact of each source calculated by BL16-SRC01, shown in Figure 4b, led to an increase in $\text{NO}_3^- + \text{NO}_2^-$ -N yields in the agricultural regions, specifically west-central UMRB (HUC 0702, 0708, and 0710), primarily due to increasing $\text{NO}_3^- + \text{NO}_2^-$ -N from manure, fertilizer, and BNF (Figures S10–S12). Changes in agricultural sources had distinct patterns, with manure impacts concentrated in regions 0708 and 0710 (Figure S10), while fertilizer applications drove substantial increases in regions 0708, 0710, and 0702 (Figure S11). Point source impacts from WWTP were particularly

significant in urban regions, creating localized hotspots of increased $\text{NO}_3^- + \text{NO}_2^-$ -N yield change (Figure S8).

Hydrological impacts (NT01-BL01, Figure 4c) increased $\text{NO}_3^- + \text{NO}_2^-$ -N yields in the central part of the UMRB (HUC 0702, 0708, 0709, 0710, 0712, and 0713) because of the increases in precipitation (NT01-PRCP01), as shown in Figure S16. Temperature effects (PRCP01-TEMP01) varied geographically (Figure S17) in the UMRB, with increases in $\text{NO}_3^- + \text{NO}_2^-$ -N yields in northern regions (0702, 0708, and 0710) and decreases in $\text{NO}_3^- + \text{NO}_2^-$ -N yields in southern areas (southern 0708, 0712, and 0713). The spatial patterns in changes in the $\text{NO}_3^- + \text{NO}_2^-$ -N suggest that the most effective conservation practices would be to consider both human activities and weather-driven mechanisms, particularly in areas where both factors contribute substantially to increased $\text{NO}_3^- + \text{NO}_2^-$ -N yields.

To better analyze the possible causes of changes in $\text{NO}_3^- + \text{NO}_2^-$ -N yields and develop possible strategies to reduce regional nutrient loss, the decomposition was aggregated into HUC04 subregions (codes and names in Table S6), as shown in Figure 5. For the entire UMRB, the average HUC12 $\text{NO}_3^- + \text{NO}_2^-$ -N yield increased by 9.7 kg/ha/yr from 2001–2005 and 2016–2020, with anthropogenic effects accounting for 4.8 kg/ha/yr of the change. At the HUC04 scale, 0708 and 0710 had the largest increase in $\text{NO}_3^- + \text{NO}_2^-$ -N yields (24.0 and 17.3 kg/ha/yr), with anthropogenic effects contributing 11.0 and 8.4 kg/ha/yr, respectively.

The aggregation to the HUC04 scale provides insights into the spatial variation in the dominant anthropogenic factors across different HUC04 subregions (Figure 5). Fertilizer and manure were primary drivers in subregions 0706, 0708, and 0710. Urban sources, including WWTP and urban nonpoint sources, were dominant in 0701 and 0712. Increasing CRP area was associated with reductions in $\text{NO}_3^- + \text{NO}_2^-$ -N yields in subregions 0708 and 0710, while increasing no-till practices facilitated nitrogen transport in these two subregions. The hydrological impacts were dominant in 0709, 0712, and 0713, accounting for more than 65% of the change in the $\text{NO}_3^- + \text{NO}_2^-$ -N yield change. This pattern aligns with the observed

increase in precipitation during the study period in these areas (Figure S19), which likely intensified nitrogen transport.

To assess the robustness of our findings against potential biases in period selection (i.e., 2001–2005 and 2016–2020), a comprehensive sensitivity analysis was conducted using multiple temporal comparison windows with the SPARROW model calibrated using 20-year data (Figures S20–S29). This analysis evaluated five alternative period pairs: 2001–2006 vs 2015–2020, 2001–2007 vs 2014–2020, 2001–2008 vs 2013–2020, 2001–2009 vs 2012–2020, and 2001–2010 vs 2011–2020. These alternative temporal comparisons consistently reproduced the primary spatial patterns and driver attributions observed in our main analysis, confirming that our findings were not artifacts of the specific time periods selected.

4. DISCUSSION

4.1. What are the Key Spatiotemporal Patterns of Riverine $\text{NO}_3^- + \text{NO}_2^-$ -N Export in the UMRB? Our spatial patterns and SPARROW model coefficients align with previous research on the dominant drivers of nitrogen export in the UMRB and broader Midwest region. The estimated source coefficients are comparable to those reported in earlier SPARROW applications, including studies of the Illinois River Basin,⁵⁴ the UMRB,¹⁷ the MARB,^{11,55} and the Great Lakes region.^{56,57} The positive effects of precipitation, tile drainage, clay content, and no-till practices on nitrogen delivery, as well as the negative effects of CRP and temperature, are consistent with the relationships observed in these earlier studies. A higher stream attenuation rate under low-discharge conditions is also identified in the UMRB study,¹⁷ and the magnitude of the reservoir attenuation coefficient is comparable to those found in both the UMRB¹⁷ and MARB⁵⁵ analyses. In terms of spatial distribution, the $\text{NO}_3^- + \text{NO}_2^-$ -N export hotspots in central UMRB are consistent with previous findings from both modeling⁵⁸ and observational analyses.²⁰ WRTDS-K annual load estimates align well with those from the USGS National Water Quality Network (NWQN),⁵⁹ supporting their validity for SPARROW calibration. Our analysis demonstrated spatiotemporal variations in $\text{NO}_3^- + \text{NO}_2^-$ -N export across the UMRB during 2001–2020. The northern, central, and parts of the eastern UMRB experienced substantial increases in $\text{NO}_3^- + \text{NO}_2^-$ -N yields, while the southern regions showed more variable changes.

This study identifies temporal variations that were not captured in previous static SPARROW models for this area.¹¹ Results of this study indicate that the increase in $\text{NO}_3^- + \text{NO}_2^-$ -N yields in the northern and central UMRB was primarily driven by agricultural sources, including increased fertilizer and manure applications and expanded planting of nitrogen-fixing crops, and increased precipitation, which aligns with earlier studies highlighting the role of agricultural intensification and precipitation patterns in amplifying nitrogen losses through leaching and runoff.^{20,58,60–63} The decline in $\text{NO}_3^- + \text{NO}_2^-$ -N yields in the southern part of the UMRB was likely associated with the implementation of agricultural conservation practices and air quality regulations.

While this study focused exclusively on $\text{NO}_3^- + \text{NO}_2^-$ -N, future work could extend the modeling framework to total nitrogen or other species (i.e., phosphorus) for a better understanding of nutrient dynamics. Although the SPARROW model demonstrated strong overall performance, further refinement of the model may provide better estimates in

high-yield areas. In addition, future work could explore the seasonality and legacy effects on nitrogen export, such as examined by Schmadel et al.⁵⁴

4.2. What are the Key Drivers Affecting $\text{NO}_3^- + \text{NO}_2^-$ -N Export Patterns? The temporal evolution of $\text{NO}_3^- + \text{NO}_2^-$ -N source contributions identified the drivers of nutrient export and also shed light on addressing the challenges of intensified agricultural inputs in reducing overall nutrient loads. The source contributions demonstrated an agreement with previous studies that agricultural sources, including fertilizer, manure, and BNF, account for more than 50% of nitrogen export.^{11,38} The consistent dominance of manure raises concerns about the ongoing expansion of livestock production,⁶⁴ suggesting the importance of improving its management strategies. The relative contribution and absolute load from fertilizers have increased, aligning with previous work^{11,55} and reflecting that there are potential opportunities in nutrient loss reductions through improved nutrient management practices. While urban sources contributed a relatively small share overall, their increasing influence emphasizes the potential importance of targeted attention and management.

Previous research attempted to compare source contributions throughout the MARB between 2002 and 2012 using results derived from different SPARROW models.¹¹ However, those comparisons were limited by variations in data sources, model structures, and inputs between different model implementations, making direct temporal comparisons challenging. This study overcomes these limitations by applying a single, consistent SPARROW model framework from 2001 to 2020, ensuring that the observed changes reflect actual shifts in nitrogen dynamics rather than methodological differences.

4.3. What are the Implications of Separating Anthropogenic and Hydrological Impacts for Developing Targeted Nutrient Reduction Strategies? Using a scenario-based modeling framework, the effects of anthropogenic activities and hydrological variability on the $\text{NO}_3^- + \text{NO}_2^-$ -N yield changes were separated. The granularity of analysis at the HUC12 level provides valuable insights for designing more efficient and effective nutrient reduction strategies that were previously obscured in broader-scale assessments. Regions where anthropogenic drivers, particularly manure, fertilizer, or urban sources, exert a dominant influence may be reduced by targeted conservations, such as precision fertilization, enhanced manure management, or upgrades to wastewater treatment facilities.^{65–67} Areas experiencing substantial hydrologically driven increases in nitrogen export may benefit from improved drainage management, reservoir construction, and wetland and floodplain restoration.^{68,69} Future research could incorporate scenarios that would enhance our understanding of nitrogen export patterns under varying hydrological conditions.

The complex role of conservation practices further highlights the potential of adaptive strategies. Practices like CRP and no-till can have contrasting effects depending on local soils, landforms, and climate regimes. The positive relationship between no-till practices and nitrogen transport observed in our study is supported by recent research,^{34,70,71} which demonstrates that no-till practices may enhance nitrogen delivery in the UMRB. Cover crop adoption was not statistically significant in our SPARROW model, which may be because the adoption rate was still low in the UMRB, typically ranging from only 2 to 4% in most of counties.^{72,73}

These findings advocate for a watershed-specific blend of best management practices that collectively address both human-induced and weather-induced drivers of nitrogen loading. By integrating scenario-based modeling and stakeholder engagement, conservation practitioners, including farmers, conservation specialists, and watershed managers, can prioritize conservations that have the most effective water-quality improvements in each subregion of the UMRB. Our approach complements and extends existing state-level nutrient reduction strategies,^{74–76} which estimated nutrient loads and set reduction goals based on monitoring data at major USGS gaging stations. While those strategies provide valuable basin-scale assessments, they are spatially coarse and may overlook important subwatershed-level variation. By contrast, our high-resolution modeling at the HUC12 scale offers more granular insight into where specific sources dominate and which conservation practices may be the most applicable. In addition, extending this framework to include other nutrients and expanding spatial coverage would provide a more comprehensive understanding of nutrient dynamics in the entire MARB and potentially in other major river basins.

Overall, this study introduces a methodological advancement by applying the SPARROW framework at an annual time step and integrating scenario-based attribution to disentangle anthropogenic and hydrological controls on nitrogen export across a large river basin. The separation of human and climatic influences provides a scientific foundation for targeted, adaptive watershed management, allowing policymakers and conservation programs to prioritize actions based on the dominant drivers in each subregion.

ASSOCIATED CONTENT

Supporting Information

The Supporting Information is available free of charge at <https://pubs.acs.org/doi/10.1021/acs.est.5c06476>.

Detailing the structure of the SPARROW model and WRTDS-K, input data, and validation methods (Texts S1–S5); additional tables describing input variables, model calibration results, monitoring sites, and HUC4 subregions (Tables S1–S6); and 29 supporting figures (Figures S1–S29) illustrating model performance, nitrogen yield spatial distributions, source contributions, and decomposition results across different time periods and subregions of the UMRB ([PDF](#))

AUTHOR INFORMATION

Corresponding Authors

Bin Peng — Agroecosystem Sustainability Center, Institute for Sustainability, Energy, and Environment, University of Illinois Urbana–Champaign, Urbana, Illinois 61820, United States; Department of Crop Sciences, College of Agricultural, Consumer and Environmental Sciences, DOE Center for Advanced Bioenergy and Bioproducts Innovation, and National Center for Supercomputing Applications, University of Illinois Urbana–Champaign, Urbana, Illinois 61820, United States; Email: binpeng@illinois.edu

Kaiyu Guan — Agroecosystem Sustainability Center, Institute for Sustainability, Energy, and Environment, University of Illinois Urbana–Champaign, Urbana, Illinois 61820, United States; Department of Natural Resources and Environmental Sciences, College of Agricultural, Consumer and Environmental Sciences, DOE Center for Advanced Bioenergy

and Bioproducts Innovation, and National Center for Supercomputing Applications, University of Illinois Urbana–Champaign, Urbana, Illinois 61820, United States; Email: kaiyug@illinois.edu

Authors

Qianyu Zhao — Agroecosystem Sustainability Center, Institute for Sustainability, Energy, and Environment, University of Illinois Urbana–Champaign, Urbana, Illinois 61820, United States; Department of Natural Resources and Environmental Sciences, College of Agricultural, Consumer and Environmental Sciences, University of Illinois Urbana–Champaign, Urbana, Illinois 61820, United States;  orcid.org/0000-0003-4256-4843

Zewei Ma — Agroecosystem Sustainability Center, Institute for Sustainability, Energy, and Environment, University of Illinois Urbana–Champaign, Urbana, Illinois 61820, United States; Department of Natural Resources and Environmental Sciences, College of Agricultural, Consumer and Environmental Sciences and DOE Center for Advanced Bioenergy and Bioproducts Innovation, University of Illinois Urbana–Champaign, Urbana, Illinois 61820, United States

Mengqi Jia — Agroecosystem Sustainability Center, Institute for Sustainability, Energy, and Environment, University of Illinois Urbana–Champaign, Urbana, Illinois 61820, United States;  orcid.org/0000-0003-2824-4747

Gregory F. McIsaac — Department of Natural Resources and Environmental Sciences, College of Agricultural, Consumer and Environmental Sciences, University of Illinois Urbana–Champaign, Urbana, Illinois 61820, United States

Dale M. Robertson — U.S. Geological Survey, Madison, Wisconsin 53726, United States

David A. Saad — U.S. Geological Survey, Madison, Wisconsin 53726, United States

Richard E. Warner — Department of Natural Resources and Environmental Sciences, College of Agricultural, Consumer and Environmental Sciences, University of Illinois Urbana–Champaign, Urbana, Illinois 61820, United States; National Great Rivers Research and Education Center, East Alton, Illinois 62024, United States

Xiaocui Wu — Agroecosystem Sustainability Center, Institute for Sustainability, Energy, and Environment, University of Illinois Urbana–Champaign, Urbana, Illinois 61820, United States; DOE Center for Advanced Bioenergy and Bioproducts Innovation, University of Illinois Urbana–Champaign, Urbana, Illinois 61820, United States

Qu Zhou — Agroecosystem Sustainability Center, Institute for Sustainability, Energy, and Environment, University of Illinois Urbana–Champaign, Urbana, Illinois 61820, United States; Department of Natural Resources and Environmental Sciences, College of Agricultural, Consumer and Environmental Sciences, University of Illinois Urbana–Champaign, Urbana, Illinois 61820, United States

Complete contact information is available at: <https://pubs.acs.org/10.1021/acs.est.5c06476>

Notes

The authors declare no competing financial interest.

ACKNOWLEDGMENTS

This research was partially supported by NSF Signals in the Soil (SiS) program (award #: 2034385), NSF Smart-Connected Community (award #: 2125626), NSF Career

Award (award #: 1847334), USDA Hatch, USDA NIFA (award #: 2023-67013-39046), and Illinois Nutrient Research and Education Council (NREC) (award #: 2026-3-360558-231). This work was also partially funded by the DOE Center for Advanced Bioenergy and Bioproducts Innovation (U.S. Department of Energy, Office of Science, Biological and Environmental Research Program under Award Number DE-SC0018420). Any opinions, findings, and conclusions or recommendations expressed in this publication are those of the author(s) and do not necessarily reflect the views of the U.S. Department of Energy. We also acknowledge the support from the Dudley Smith Initiative in the College of Agricultural, Consumer and Environmental Sciences at the University of Illinois Urbana–Champaign.

■ REFERENCES

- (1) Bouwman, L.; Goldewijk, K. K.; Van Der Hoek, K. W.; Beusen, A. H. W.; Van Vuuren, D. P.; Willem, J.; Rufino, M. C.; Stehfest, E. Exploring Global Changes in Nitrogen and Phosphorus Cycles in Agriculture Induced by Livestock Production over the 1900–2050 Period. *Proc. Natl. Acad. Sci. U.S.A.* **2013**, *110* (52), 20882–20887.
- (2) Leavitt, S. W. Biogeochemistry, an Analysis of Global Change. *Eos, Trans., Am. Geophys. Union* **1998**, *79* (2), 20.
- (3) Li, L.; Knapp, J. L. A.; Lintern, A.; Ng, G.-H. C.; Perdrial, J.; Sullivan, P. L.; Zhi, W. River Water Quality Shaped by Land–river Connectivity in a Changing Climate. *Nat. Clim. Chang.* **2024**, *14* (3), 225–237.
- (4) Robertson, G. P.; Vitousek, P. M. Nitrogen in Agriculture: Balancing the Cost of an Essential Resource. *Annu. Rev. Environ. Resour.* **2009**, *34* (1), 97–125.
- (5) Withers, P.; Neal, C.; Jarvie, H.; Doody, D. Agriculture and Eutrophication: Where Do We Go from Here? *Sustainability* **2014**, *6* (9), 5853–5875.
- (6) Dodds, W. K.; Bouska, W. W.; Eitzmann, J. L.; Pilger, T. J.; Pitts, K. L.; Riley, A. J.; Schloesser, J. T.; Thornbrugh, D. J. Eutrophication of U.S. Freshwaters: Analysis of Potential Economic Damages. *Environ. Sci. Technol.* **2009**, *43* (1), 12–19.
- (7) Paerl, H. W.; Hall, N. S.; Calandino, E. S. Controlling Harmful Cyanobacterial Blooms in a World Experiencing Anthropogenic and Climatic-Induced Change. *Sci. Total Environ.* **2011**, *409* (10), 1739–1745.
- (8) Cheng, F. Y.; Van Meter, K. J.; Byrnes, D. K.; Basu, N. B. Maximizing US Nitrate Removal through Wetland Protection and Restoration. *Nature* **2020**, *588* (7839), 625–630.
- (9) Anderson, D. M.; Glibert, P. M.; Burkholder, J. M. Harmful Algal Blooms and Eutrophication: Nutrient Sources, Composition, and Consequences. *Estuaries* **2002**, *25* (4), 704–726.
- (10) Lu, C.; Zhang, J.; Yi, B.; Calderon, I.; Feng, H.; Miao, R.; Hennessy, D.; Pan, S.; Tian, H. Riverine Nitrogen Footprint of Agriculture in the Mississippi–Atchafalaya River Basin: Do We Trade Water Quality for Crop Production? *Environ. Res. Lett.* **2023**, *18* (11), No. 114043.
- (11) Robertson, D. M.; Saad, D. A. Nitrogen and Phosphorus Sources and Delivery from the Mississippi/Atchafalaya River Basin: An Update Using 2012 SPARROW Models. *J. Am. Water Resour. Assoc.* **2021**, *57* (3), 406–429.
- (12) Smith, V. H.; Tilman, G. D.; Nekola, J. C. Eutrophication: Impacts of Excess Nutrient Inputs on Freshwater, Marine, and Terrestrial Ecosystems. *Environ. Pollut.* **1999**, *100* (1–3), 179–196.
- (13) Michalak, A. M.; Anderson, E. J.; Beletsky, D.; Boland, S.; Bosch, N. S.; Bridgeman, T. B.; Chaffin, J. D.; Cho, K.; Confesor, R.; Daloglu, I.; Depinto, J. V.; Evans, M. A.; Fahnstiel, G. L.; He, L.; Ho, J. C.; Jenkins, L.; Johengen, T. H.; Kuo, K. C.; Laporte, E.; Liu, X.; McWilliams, M. R.; Moore, M. R.; Posselt, D. J.; Richards, R. P.; Scavia, D.; Steiner, A. L.; Verhamme, E.; Wright, D. M.; Zagorski, M. A. Record-Setting Algal Bloom in Lake Erie Caused by Agricultural and Meteorological Trends Consistent with Expected Future Conditions. *Proc. Natl. Acad. Sci. U.S.A.* **2013**, *110* (16), 6448–6452.
- (14) Pretty, J. N.; Mason, C. F.; Nedwell, D. B.; Hine, R. E.; Leaf, S.; Dils, R. Environmental Costs of Freshwater Eutrophication in England and Wales. *Environ. Sci. Technol.* **2003**, *37* (2), 201–208.
- (15) Van Meter, K. J.; Van Cappellen, P.; Basu, N. B. Legacy Nitrogen May Prevent Achievement of Water Quality Goals in the Gulf of Mexico. *Science* **2018**, *360* (6387), 427–430.
- (16) Smith, R. A.; Alexander, R. B.; Schwarz, G. E. Natural Background Concentrations of Nutrients in Streams and Rivers of the Conterminous United States. *Environ. Sci. Technol.* **2003**, *37* (14), 3039–3047.
- (17) García, A. M.; Alexander, R. B.; Arnold, J. G.; Norfleet, L.; White, M. J.; Robertson, D. M.; Schwarz, G. Regional Effects of Agricultural Conservation Practices on Nutrient Transport in the Upper Mississippi River Basin. *Environ. Sci. Technol.* **2016**, *50* (13), 6991–7000.
- (18) Marinos, R. E.; Van Meter, K. J.; Basu, N. B. Is the River a Chemostat?: Scale versus Land Use Controls on Nitrate Concentration-discharge Dynamics in the Upper Mississippi River Basin. *Geophys. Res. Lett.* **2020**, *47* (16), No. e2020GL087051.
- (19) Burkart, M. R.; James, D. E. Agricultural-nitrogen Contributions to Hypoxia in the Gulf of Mexico. *J. Environ. Qual.* **1999**, *28* (3), 850–859.
- (20) David, M. B.; Drinkwater, L. E.; McIsaac, G. F. Sources of Nitrate Yields in the Mississippi River Basin. *J. Environ. Qual.* **2010**, *39* (5), 1657–1667.
- (21) Diaz, R. J.; Rosenberg, R. Spreading Dead Zones and Consequences for Marine Ecosystems. *Science* **2008**, *321* (5891), 926–929.
- (22) Rabalais, N. N.; Turner, R. E.; Wiseman, W. J., Jr. Gulf of Mexico Hypoxia, A.k.a. “the Dead Zone”. *Annu. Rev. Ecol. Syst.* **2002**, *33* (1), 235–263.
- (23) US-EPA. Mississippi River/Gulf of Mexico Hypoxia Task Force. 2014.
- (24) Alexander, R. B.; Boyer, E. W.; Smith, R. A.; Schwarz, G. E.; Moore, R. B. The Role of Headwater Streams in Downstream Water Quality. *J. Am. Water Resour. Assoc.* **2007**, *43* (1), 41–59.
- (25) Alexander, R. B.; Smith, R. A.; Schwarz, G. E.; Boyer, E. W.; Nolan, J. V.; Brakebill, J. W. Differences in Phosphorus and Nitrogen Delivery to the Gulf of Mexico from the Mississippi River Basin. *Environ. Sci. Technol.* **2008**, *42* (3), 822–830.
- (26) McIsaac, G. F.; David, M. B.; Gerter, G. Z.; Goolsby, D. A. Nitrate Flux in the Mississippi River. *Nature* **2001**, *414* (6860), 166–167.
- (27) Sinha, E.; Michalak, A. M.; Balaji, V. Eutrophication Will Increase during the 21st Century as a Result of Precipitation Changes. *Science* **2017**, *357* (6349), 405–408.
- (28) Bieroza, M.; Acharya, S.; Benisch, J.; ter Borg, R. N.; Hallberg, L.; Negri, C.; Pruitt, A.; Pucher, M.; Saavedra, F.; Staniszewska, K.; van’t Veen, S. G. M.; Vincent, A.; Winter, C.; Basu, N. B.; Jarvie, H. P.; Kirchner, J. W. Advances in Catchment Science, Hydrochemistry, and Aquatic Ecology Enabled by High-Frequency Water Quality Measurements. *Environ. Sci. Technol.* **2023**, *57* (12), 4701–4719.
- (29) Pellerin, B. A.; Bergamaschi, B. A.; Gilliom, R. J.; Crawford, C. G.; Saraceno, J.; Frederick, C. P.; Downing, B. D.; Murphy, J. C. Mississippi River Nitrate Loads from High Frequency Sensor Measurements and Regression-Based Load Estimation. *Environ. Sci. Technol.* **2014**, *48* (21), 12612–12619.
- (30) Mohammed, H.; Hansen, A. T. Spatial Heterogeneity of Low Flow Hydrological Alterations in Response to Climate and Land Use within the Upper Mississippi River Basin. *J. Hydrol.* **2024**, *632*, No. 130872.
- (31) Daggupati, P.; Yen, H.; White, M. J.; Srinivasan, R.; Arnold, J. G.; Keitzer, C. S.; Sowa, S. P. Impact of Model Development, Calibration and Validation Decisions on Hydrological Simulations in West Lake Erie Basin: Impact of Model Development Decisions on Streamflow Simulations. *Hydrol. Process.* **2015**, *29* (26), 5307–5320.

(32) Sehgal, V.; Sridhar, V. Watershed-Scale Retrospective Drought Analysis and Seasonal Forecasting Using Multi-Layer, High-Resolution Simulated Soil Moisture for Southeastern U.S. *Weather Clim. Extrem.* **2019**, *23*, No. 100191.

(33) McIsaac, G. F.; Hodson, T. O.; Markus, M.; Bhattacharai, R.; Kim, D. C. Spatial and Temporal Variations in Phosphorus Loads in the Illinois River Basin, Illinois USA. *J. Am. Water Resour. Assoc.* **2023**, *59* (3), 523–538.

(34) Stackpoole, S.; Sabo, R.; Falcone, J.; Sprague, L. Long-Term Mississippi River Trends Expose Shifts in the River Load Response to Watershed Nutrient Balances Between 1975 and 2017. *Water Resour. Res.* **2021**, *57* (11), No. e2021WR030318.

(35) Sprague, L. A.; Hirsch, R. M.; Aulenbach, B. T. Nitrate in the Mississippi River and Its Tributaries, 1980 to 2008: Are We Making Progress? *Environ. Sci. Technol.* **2011**, *45* (17), 7209–7216.

(36) Murphy, J. C.; Hirsch, R. M.; Sprague, L. A. *Scientific Investigations Report, Nitrate in the Mississippi River and Its Tributaries, 1980–2010: An Update*; U.S. Geological Survey, 2013.

(37) Botero-Acosta, A.; McIsaac, G. F.; Gilinsky, E.; Warner, R.; Lee, J. S. Nitrate-N Trends in Mississippi and Atchafalaya River Basin Watersheds: Exploring Correlations of Watershed Features with Nutrient Trends Components 2000–2020. *Sci. Total Environ.* **2025**, *970*, No. 179042.

(38) Robertson, D. M.; Saad, D. A.; Schwarz, G. E. Spatial Variability in Nutrient Transport by HUC8, State, and Subbasin Based on Mississippi/Atchafalaya River Basin SPARROW Models. *J. Am. Water Resour. Assoc.* **2014**, *50* (4), 988–1009.

(39) Musolff, A.; Zhan, Q.; Dupas, R.; Minaudo, C.; Fleckenstein, J. H.; Rode, M.; Dehaspe, J.; Rinke, K. Spatial and Temporal Variability in Concentration-Discharge Relationships at the Event Scale. *Water Resour. Res.* **2021**, *57* (10), No. e2020WR029442.

(40) Qi, J.; Zhang, X.; Yang, Q.; Srinivasan, R.; Arnold, J. G.; Li, J.; Waldhoff, S. T.; Cole, J. SWAT Ungauged: Water Quality Modeling in the Upper Mississippi River Basin. *J. Hydrol.* **2020**, *584*, No. 124601.

(41) Pandit, A.; Golden, H. E.; Christensen, J. R.; Lane, C. R.; Husic, A. Deep Learning Prediction and Interpretation of Riverine Nitrate Export Across the Mississippi River Basin. *Water Resour. Res.* **2025**, *61* (8), No. e2024WR039207.

(42) Tomer, M. D.; Locke, M. A. The Challenge of Documenting Water Quality Benefits of Conservation Practices: A Review of USDA-ARS's Conservation Effects Assessment Project Watershed Studies. *Water Sci. Technol.* **2011**, *64* (1), 300–310.

(43) Han, H.; Allan, J. D.; Scavia, D. Influence of Climate and Human Activities on the Relationship between Watershed Nitrogen Input and River Export. *Environ. Sci. Technol.* **2009**, *43* (6), 1916–1922.

(44) Choquette, A. F.; Hirsch, R. M.; Murphy, J. C.; Johnson, L. T.; Confesor, R. B., Jr. Tracking Changes in Nutrient Delivery to Western Lake Erie: Approaches to Compensate for Variability and Trends in Streamflow. *J. Great Lakes Res.* **2019**, *45* (1), 21–39.

(45) Zhi, W.; Baniecki, H.; Liu, J.; Boyer, E.; Shen, C.; Shenk, G.; Liu, X.; Li, L. Increasing Phosphorus Loss despite Widespread Concentration Decline in US Rivers. *Proc. Natl. Acad. Sci. U.S.A.* **2024**, *121* (48), No. e2402028121.

(46) Uniyal, B.; Kosatka, E.; Koellner, T. Spatial and Temporal Variability of Climate Change Impacts on Ecosystem Services in Small Agricultural Catchments Using the Soil and Water Assessment Tool (SWAT). *Sci. Total Environ.* **2023**, *875*, No. 162520.

(47) Homer, C.; Dewitz, J.; Yang, L.; Jin, S.; Danielson, P.; Xian, G.; Coulston, J.; Herold, N.; Wickham, J.; Megown, K. Completion of the 2011 National Land Cover Database for the Conterminous United States—Representing a Decade of Land Cover Change Information. *Photogramm. Eng. Remote Sens.* **2015**, *81* (5), 345–354.

(48) Zhang, Q.; Hirsch, R. M. River Water-Quality Concentration and Flux Estimation Can Be Improved by Accounting for Serial Correlation Through an Autoregressive Model. *Water Resour. Res.* **2019**, *55* (11), 9705–9723.

(49) Smith, R. A.; Schwarz, G. E.; Alexander, R. B. Regional Interpretation of Water-quality Monitoring Data. *Water Resour. Res.* **1997**, *33* (12), 2781–2798.

(50) Schwarz, G. E.; Hoos, A. B.; Alexander, R. B.; Smith, R. A. The SPARROW Surface Water-Quality Model: Theory, Application and User Documentation. In *U.S. Geological Survey Techniques and Methods Report*; U.S. Geological Survey: Reston, VA, 2006.

(51) Sekellick, A. J.; Sherr, C. E. Nitrogen and phosphorus inputs from fertilizer and manure in the Continental United States, 2002–2017. U.S. Geological Survey data release. <https://www.sciencebase.gov/catalog/item/65787037d34e952b22746538> (accessed February 03, 2025).

(52) Brakebill, J. W.; Gronberg, J. A. M. County-Level Estimates of Nitrogen and Phosphorus from Commercial Fertilizer for the Conterminous United States, 1987–2012. U.S. Geological Survey data release. <https://www.sciencebase.gov/catalog/item/5851b2d1e4b0f99207c4f238> (accessed February 03, 2025).

(53) PRISM Climate Group, Oregon State University. PRISM Gridded Climate Data. <https://prism.oregonstate.edu> (accessed February 03, 2025).

(54) Schmadel, N. M.; Miller, O. L.; Ator, S. W.; Miller, M. P.; Schwarz, G. E.; Robertson, D. M.; Sekellick, A. J.; Skinner, K. D.; Saad, D. A. Seasonally Varying Contributions of Contemporaneous and Lagged Sources of Instream Total Nitrogen and Phosphorus Load across the Illinois River Basin. *Sci. Total Environ.* **2024**, *955*, No. 176816.

(55) Robertson, D. M.; Saad, D. A. SPARROW Models Used to Understand Nutrient Sources in the Mississippi/Atchafalaya River Basin. *J. Environ. Qual.* **2013**, *42* (5), 1422–1440.

(56) Robertson, D. M.; Saad, D. A. Nutrient Inputs to the Laurentian Great Lakes by Source and Watershed Estimated Using SPARROW Watershed Models: Nutrient Inputs to the Laurentian Great Lakes by Source and Watershed Estimated Using SPARROW Watershed Models. *J. Am. Water Resour. Assoc.* **2011**, *47* (5), 1011–1033.

(57) Robertson, D. M.; Saad, D. A.; Benoy, G. A.; Vouk, I.; Schwarz, G. E.; Laitta, M. T. Phosphorus and Nitrogen Transport in the Binational Great Lakes Basin Estimated Using SPARROW Watershed Models. *J. Am. Water Resour. Assoc.* **2019**, *55* (6), 1401–1424.

(58) Tian, H.; Xu, R.; Pan, S.; Yao, Y.; Bian, Z.; Cai, W.-J.; Hopkinson, C. S.; Justic, D.; Lohrenz, S.; Lu, C.; Ren, W.; Yang, J. Long-term Trajectory of Nitrogen Loading and Delivery from Mississippi River Basin to the Gulf of Mexico. *Global Biogeochem. Cycles* **2020**, *34* (5), No. e2019GB006475.

(59) Lee, C. Nutrient and pesticide data collected from the USGS National Water Quality Network and previous networks, 1950–2022. U.S. Geological Survey data release. <https://www.sciencebase.gov/catalog/item/655d2063d34ee4b6e05cc9e6> (accessed August 05, 2024).

(60) Sinha, E.; Michalak, A. M.; Calvin, K. V.; Lawrence, P. J. Societal Decisions about Climate Mitigation Will Have Dramatic Impacts on Eutrophication in the 21st Century. *Nat. Commun.* **2019**, *10* (1), No. 939.

(61) McCrackin, M. L.; Harrison, J. A.; Compton, J. E. Future Riverine Nitrogen Export to Coastal Regions in the United States: Prospects for Improving Water Quality. *J. Environ. Qual.* **2015**, *44* (2), 345–355.

(62) Zhang, J.; Lu, C.; Crumpton, W.; Jones, C.; Tian, H.; Villarini, G.; Schilling, K.; Green, D. Heavy Precipitation Impacts on Nitrogen Loading to the Gulf of Mexico in the 21st Century: Model Projections under Future Climate Scenarios. *Earths Future* **2022**, *10* (4), No. e2021EF002141.

(63) Sabo, R. D.; Clark, C. M.; Compton, J. E. Considerations When Using Nutrient Inventories to Prioritize Water Quality Improvement Efforts across the US. *Environ. Res. Commun.* **2021**, *3* (4), No. 045005.

(64) Walljasper, C. Large animal feeding operations on the rise Investigate Midwest. <http://investigatemidwest.org/2018/06/07/>

large-animal-feeding-operations-on-the-rise-2/ (accessed April 03, 2025).

(65) Deng, O.; Wang, S.; Ran, J.; Huang, S.; Zhang, X.; Duan, J.; Zhang, L.; Xia, Y.; Reis, S.; Xu, J.; Xu, J.; de Vries, W.; Sutton, M. A.; Gu, B. Managing Urban Development Could Halve Nitrogen Pollution in China. *Nat. Commun.* **2024**, *15* (1), No. 401.

(66) Torres-Martinez, J. A.; Mahlknecht, J.; Mora, A.; Kaown, D.; Koh, D.-C.; Mayer, B.; Tetzlaff, D. Unveiling Nitrate Origins in Semiarid Aquifers: A Comparative Analysis of Bayesian Isotope Mixing Models Using Nitrate and Boron Isotopes and a Positive Matrix Factorization Model. *J. Hydrol.* **2024**, *639*, No. 131622.

(67) Zhao, Y.-L.; Sun, H.-J.; Wang, X.-D.; Ding, J.; Lu, M.-Y.; Pang, J.-W.; Zhou, D.-P.; Liang, M.; Ren, N.-Q.; Yang, S.-S. Spatiotemporal Drivers of Urban Water Pollution: Assessment of 102 Cities across the Yangtze River Basin. *Environ. Sci. Technol.* **2024**, *20*, No. 100412.

(68) Salk, K. R.; Steinman, A. D.; Ostrom, N. E. Wetland Restoration and Hydrologic Reconnection Result in Enhanced Watershed Nitrogen Retention and Removal. *Wetlands* **2018**, *38* (2), 349–359.

(69) Steidl, J.; Kaletka, T.; Bauwe, A. Nitrogen Retention Efficiency of a Surface-Flow Constructed Wetland Receiving Tile Drainage Water: A Case Study from North-Eastern Germany. *Agric. Ecosyst. Environ.* **2019**, *283*, No. 106577.

(70) Huang, Y.; Ren, W.; Lindsey, L. E.; Wang, L.; Hui, D.; Tao, B.; Jacinth, P.-A.; Tian, H. No-Tillage Farming Enhances Widespread Nitrate Leaching in the US Midwest. *Environ. Res. Lett.* **2024**, *19* (10), No. 104062.

(71) Liang, K.; Zhang, X.; McCarty, G. W.; Zhao, K.; Gao, F. From Basin to Gulf: Conservation Tillage Improves Soil Health but Exacerbates Hypoxia. *NPJ Sustainable Agric.* **2025**, *3* (1), No. 47.

(72) Zhou, Q.; Guan, K.; Wang, S.; Jiang, C.; Huang, Y.; Peng, B.; Chen, Z.; Wang, S.; Hippel, J.; Schaefer, D.; Qin, Z.; Stroebel, S.; Coppess, J.; Khanna, M.; Cai, Y. Recent Rapid Increase of Cover Crop Adoption across the U.S. Midwest Detected by Fusing Multi-source Satellite Data. *Geophys. Res. Lett.* **2022**, *49* (22), No. e2022GL100249.

(73) Deines, J. M.; Guan, K.; Lopez, B.; Zhou, Q.; White, C. S.; Wang, S.; Lobell, D. B. Recent Cover Crop Adoption Is Associated with Small Maize and Soybean Yield Losses in the United States. *Glob. Change Biol.* **2023**, *29* (3), 794–807.

(74) Iowa Department of Agriculture and Land Stewardship; Iowa Department of Natural Resources. Iowa State University College of Agriculture and Life Sciences, Iowa Nutrient Reduction Strategy 2025 <https://www.nutrientstrategy.iastate.edu/sites/default/files/documents/2025%20INRS%20Complete%20Feb%202025.pdf> (accessed 2025–08–20).

(75) IEPA; IDOA; University of Illinois Extension. *Illinois Nutrient Loss Reduction Strategy Biennial Report 2021–22*; Illinois Environmental Protection Agency and Illinois Department of Agriculture; Springfield, Illinois. University of Illinois Extension: Urbana, IL, 2023.

(76) Minnesota Pollution Control Agency. 5-Year Progress Report on Minnesota's Nutrient Reduction Strategy 2020 <https://www.pca.state.mn.us/sites/default/files/wq-s1-84a.pdf> (accessed August 20, 2025).



CAS BIOFINDER DISCOVERY PLATFORM™

**ELIMINATE DATA
SILOS. FIND
WHAT YOU
NEED, WHEN
YOU NEED IT.**

A single platform for relevant,
high-quality biological and
toxicology research

Streamline your R&D

CAS
A division of the
American Chemical Society